

# Reactive amphiphilic aprotic ionic liquids based on functionalized oligomeric silsesquioxanes

Valery V. Shevchenko,<sup>\*1</sup> and Mariana Gumenna,<sup>1</sup> and Hansol Lee,<sup>2</sup> and Nina Klimenko,<sup>1</sup> and Oleksandr Stryutsky,<sup>1</sup> and Volodymyr Korolovych,<sup>2</sup> and Vladimir V. Tsukruk<sup>2</sup>

<sup>1</sup>Institute of Macromolecular Chemistry of the National Academy of Sciences of Ukraine, 48 Kharkivske Shose, Kyiv 02160, Ukraine

<sup>2</sup>School of Materials Science and Engineering, Georgia Institute of Technology, Atlanta, Georgia 30332, USA

E-mail: valpshevchenko@gmail.com



Valery V. Shevchenko

Valery V. Shevchenko is a Corresponding Member of the National Academy of Sciences of Ukraine, Professor, Head of Department of Chemistry of Oligomers and Network Polymers of Institute of Macromolecular Chemistry of the National Academy of Sciences of Ukraine. His department conducts research in the fields of synthesis of oligomeric ionic liquids of different structure and molecular architecture, organic-inorganic proton exchange membranes, photoluminescent polymeric materials and coatings. He received his M.S. degree in chemistry from the Ukrainian State University of Chemical Technology, Ph.D. degree in chemistry from Tartu State University (Estonia), and D.Sc. degree in chemistry and polymer science from the National Academy of Sciences of Ukraine.



Vladimir V. Tsukruk

Vladimir V. Tsukruk is a Regents Professor in the School of Materials Science and Engineering, Georgia Institute of Technology. His research laboratory of Surface Engineering and Molecular Assemblies, SEMA Lab conducts sustained research in the fields of polymeric nanocomposites, organic-inorganic surfaces and interfaces, directed assembly and self-assembly, natural and synthetic biopolymers, biosensors, and responsive polymers. He received his M.S. degree in Molecular Physics from the National University of Ukraine and Ph.D. and D.Sc. degrees in Chemistry and Polymer Science from the National Academy of Sciences of Ukraine. He was elected as a Fellow of American Chemical Society, American Physical Society, and Materials Research Society, is Fulbright and Humboldt Fellow, and serves as an Executive Editor of ACS Applied Materials and Interfaces.

## Abstract

A method for synthesis of organic-inorganic amphiphilic reactive aprotic cationic ionic liquids (OSS-ILs) discussed in this study includes the quaternization reaction of a mixture of oligosilsesquioxane polyhedral structures and their analogs with an open chain containing a tertiary amine and primary and secondary hydroxyl groups with n-bromopropane or n-bromodecane. Obtained compounds were amorphous with glass transition temperature below 0°C. The ionic conductivity of OSS-ILs decreases with increasing the alkyl substituent length with the maximum conductivity achieved close to  $1.4 \cdot 10^{-3}$  S/cm at 120°C.

The dynamic light scattering reveals that the length of alkyl substituent of OSS-ILs affects the assembly behavior in aqueous solutions, resulting in the formation of diverse nanoscale morphologies for the OSS-IL with longer substituent. According to atomic force microscopy images, the surface morphology of the film of OSS-IL with short substituents showed spherical flat micelles with an average diameter of  $229 \pm 92$  nm and height of 2 nm. OSS-IL with long substituents formed polydisperse complex micellar morphologies, of which a majority showed elongated, worm-like structures with an average height of 2 nm. The ability to endow ionic conductivity and to tune morphology makes these materials promising as potential polymer electrolytes for various electrochemical applications, in particular ionic sensors and energy storage devices.

## 1. Introduction

Ionic liquids are organic salts with melting point below 100 °C and that exhibit interesting physical properties, including a relatively high ionic conductivity, wide electrochemically stable window, very low vapor pressure, and high chemical and thermal stabilities.<sup>1</sup> Polymeric ionic liquids have attracted great interest due to their unique properties derived from ionic liquid composition and possibilities of practical applications as polymer electrolytes in electrochemical devices, building blocks in nanocomposites, innovative sensitive materials, and smart surfaces.<sup>2-4</sup> Oligomeric ionic liquids (OILs) occupy an intermediate position between conventional low molecular weight ionic liquids and their polymeric analogues.<sup>5, 6</sup> Combining the unique properties of ionic liquids with the peculiarities of physical behavior of oligomers, these compounds can be considered as soft ion-conducting media for various electrochemical devices, antimicrobial additives for antifouling coatings, and solvents and immobilizing agents for heterogeneous catalysis.<sup>1, 5, 6</sup>

Among OILs, polyhedral oligomeric silsesquioxanes (POSS) based OILs (POSS-ILs)<sup>7, 8</sup> with a general formula (R-SiO<sub>1.5</sub>)<sub>n</sub> where (SiO<sub>1.5</sub>)<sub>n</sub> is an inorganic completely condensed polyhedral silsesquioxane core (n = 8, 10, 12 ...) and R is an organic substituent containing ionic group are of considerable interest.<sup>9-21</sup> POSS-ILs have advantages over conventional organic OILs since the introduction of inorganic silsesquioxane core increases thermal, chemical and mechanical stability of materials,<sup>22-24</sup> and a star-like structure of POSS allows for generating an organic shell with a different number of spatially separated ionic groups for a certain functional purpose.<sup>7, 8</sup> Currently reported POSS-ILs are predominantly represented by cationic aprotic compounds.<sup>14-21</sup> Their increased density of ion-

**Keywords:** Ionic liquids, Oligomeric silsesquioxanes, Self-organization, ionic conductivity

exchange groups, high thermal and mechanical stability make them promising as dopants for anion-exchange membranes in fuel cells,<sup>14</sup> electrolytes for dye-sensitized solar cells.<sup>15</sup> The bactericidal properties of POSS-ILs open up the possibilities for creating antimicrobial<sup>18, 19, 21</sup> and antifouling<sup>20</sup> coatings, and the combination with cytocompatibility enables POSS-ILs to be used as dental filling materials.<sup>16</sup>

One of directions for further development of chemistry of such organic-inorganic OILs is to suggest the facile, one-pot synthesis of their inorganic cores. This goal can be achieved by using of a mixture of completely (cage) condensed polyhedral structures (specific to POSS) with incompletely condensed polyhedral structures and their linear and branched (open-chain) analogs.<sup>25-31</sup> The reactive mixtures have been synthesized by a sol-gel process, and the ratio of cage and open-chain structures can be regulated by changing the structure of the organic shell and the conditions for the sol-gel process.<sup>25-31</sup>

Reactive OSSs containing epoxy<sup>27, 28</sup> or methacrylate<sup>28</sup> groups as well as fragments combining aliphatic tertiary amine with hydroxyl groups (OSS(N+OH))<sup>25, 26</sup> have been synthesized. These OSSs with functional groups were considered as initial oligomers for the following polymer-analogous transformations. Despite OSS structure of the inorganic component, the obtained compounds can be referred to as branched or star-shaped<sup>32, 33</sup> compounds containing cage structures.<sup>33</sup> They are promising as building blocks for obtaining nanostructured composite materials and pH sensitive nanocomposites.<sup>34-37</sup> For example, layer-by-layer films<sup>35</sup> and microcapsules<sup>36</sup> were obtained by using OSS(N+OH)-based polymers.

Sol-gel method with trialkoxysilanes with ionic groups as initial compounds was applied to synthesize OSS-containing ionic liquids (OSS-ILs).<sup>29-31</sup> The presence of quaternary ammonium or imidazolium groups in the initial trialkoxysilanes enables the synthesis of cationic OSS-ILs.<sup>29-31</sup> These OSS-ILs contain inorganic component mainly with polyhedral (predominantly octahedral) structures or a set of various and diverse silsesquioxane structures.<sup>29-31</sup> However, to the best of our knowledge, the synthesis and properties of reactive and amphiphilic OSS-ILs have not been reported.

In order to impart the organic-inorganic OSS-ILs with new functionalities, we develop a new approach to introduce an ionic group into the organic shell of OSS in combination with reactive groups and fragments of various functionalities. This process is carried out by modifying the organic shell of OSS cores, which contain an inorganic component in the form of a mixture of initially synthesized silsesquioxane nanostructures in contrast to the currently reported methods for OSS-ILs preparation by sol-gel method with trialkoxysilanes with ionic groups.<sup>29-31</sup> This approach ensures the presence of an inorganic component and provides the possibility of further directed changes in the chemical structure and functionality of the branched organic shell.

In this work, OSS(N+OH) was chosen as an initial compound since it can contain reactive groups of various types.<sup>25</sup> The reactive groups of this compound enable both various condensation reactions and the introduction of ionic groups by direct neutralization and quaternization reactions. It should be noted that we successfully synthesized amphiphilic POSS-based polymers by using OSS(N+OH) as an initial compound.<sup>26</sup>

The aim of this work is to discuss a novel method for the synthesis of reactive amphiphilic cationic aprotic OSS-ILs containing quaternary amino groups in the organic shell in combination with hydrophobic alkyl substituents of various

lengths. The chemical structure of OSS-ILs, their ionic conductivity in the absence of moisture, and the self-organization in aqueous solutions as well as on a solid surface were investigated with focus on the effects of hydrophilic-hydrophobic properties of the compounds. It is worth noting that the self-organization of octahedral POSS-ILs has not been fully understood with a few works devoted to aprotic imidazolium-containing POSS-ILs,<sup>38-40</sup> while information on the self-organization of OSS-ILs in solution and in solid state is absent.

## 2. Experimental

**Materials.** (3-aminopropyl)triethoxysilane (99%), glycidol (96%), 1-bromopropane (99%), 1-bromodecane (98%), were purchased from Sigma-Aldrich and used as received. Dimethyl sulfoxide, acetonitrile were distilled before usage. The ultrapure water used in all experiments was prepared in a three-stage Millipore Milli-Q Plus 185 purification system (resistivity  $\geq 18.2 \text{ M}\Omega \cdot \text{cm}$ ).

**Synthesis of OSS(N+OH).** The initial compound OSS(N+OH) was synthesized according to common technique by hydrolytic condensation of the product of interaction of 3-aminopropyl triethoxysilane with a twofold molar excess of glycidol.<sup>25, 26</sup> The -OH group content was 21.4% (calcd., 25.5%). The tertiary amino group content was 4.9% (calcd. 5.4%). The amounts of the initial substances were calculated from the actual content of tertiary amino groups in OSS(N+OH). FTIR:  $\nu$  Si-O-Si (1031  $\text{cm}^{-1}$ ),  $\nu$  C-N (1097  $\text{cm}^{-1}$ ),  $\nu$  C-H bonds of CH and CH<sub>2</sub> groups (2765-3020  $\text{cm}^{-1}$ ),  $\delta$  C-H bonds of CH and CH<sub>2</sub> groups (1462  $\text{cm}^{-1}$ ),  $\nu$  O-H bonds of hydroxyl groups (3020-3723  $\text{cm}^{-1}$ ); <sup>1</sup>H NMR (400 MHz, DMSO-*d*<sub>6</sub>):  $\delta$  0.51 (2H, [SiO<sub>1.5</sub>]<sub>n</sub>CH<sub>2</sub>-), 1.50 (2H, -NCH<sub>2</sub>CH<sub>2</sub>-), 2.38 and 2.78 (6H, -NCH<sub>2</sub>-), 3.34, 3.39, 3.56, 3.71 (10H, -CH<sub>2</sub>OH, -CH(OH)-, -CH<sub>2</sub>OH, -CH(OH)-).

**Synthesis of OSS(C<sub>3</sub>N<sup>+</sup>Br<sup>-</sup>).** The solution of 1.74 g (0.0142 g-equiv) 1-bromopropane in 2 ml DMSO was added to the solution of 4.05 g (0.0142 g-equiv) OSS(N+OH) in 8 ml DMSO. The reaction was held at 80 °C and stirring for 32 h. The solvent was partially removed under reduced pressure. Then the product was precipitated and washed twice with acetonitrile. The obtained OSS(C<sub>3</sub>N<sup>+</sup>Br<sup>-</sup>) was dried at 60 °C. Yield is 4.92 g (85%). The product is a clear, light brown viscous liquid. FTIR:  $\nu$  Si-O-Si (1023  $\text{cm}^{-1}$ ),  $\nu$  C-N (1116  $\text{cm}^{-1}$ ),  $\nu$  C-H bonds of CH, CH<sub>2</sub> and CH<sub>3</sub> groups (2843-2987  $\text{cm}^{-1}$ ),  $\delta$  C-H bonds of CH, CH<sub>2</sub> and CH<sub>3</sub> groups (1463  $\text{cm}^{-1}$ ),  $\nu$  O-H bonds of hydroxyl groups (3020-3696  $\text{cm}^{-1}$ ); <sup>1</sup>H NMR (400 MHz, DMSO-*d*<sub>6</sub>):  $\delta$  0.69 (2H, [SiO<sub>1.5</sub>]<sub>n</sub>CH<sub>2</sub>-), 0.94 (3H, -CH<sub>3</sub>), 1.77 (4H, -N<sup>+</sup>CH<sub>2</sub>CH<sub>2</sub>-), 3.15, 3.37, 3.48 (16H, -N<sup>+</sup>CH<sub>2</sub>-), -CH<sub>2</sub>OH, -CH<sub>2</sub>OH, -CH(OH)-), 4.00 (2H, -CH(OH)-).

**Synthesis of OSS(C<sub>10</sub>N<sup>+</sup>Br<sup>-</sup>).** This oligomer was synthesized in a similar way to OSS(C<sub>3</sub>N<sup>+</sup>Br<sup>-</sup>). The solution of 2.37 g (0.0107 g-equiv) 1-bromodecane in 2 ml DMSO was added to the solution of 3.06 g (0.0107 g-equiv) OSS(N+OH) in 6 ml DMSO. Yield is 4.83 g (89%). The obtained OSS(C<sub>10</sub>N<sup>+</sup>Br<sup>-</sup>) is a clear, light brown viscous liquid. FTIR:  $\nu$  Si-O-Si (1043  $\text{cm}^{-1}$ ),  $\nu$  C-N (1120  $\text{cm}^{-1}$ ),  $\nu$  C-H bonds of CH, CH<sub>2</sub> and CH<sub>3</sub> groups (2832-2991  $\text{cm}^{-1}$ ),  $\delta$  C-H bonds of CH, CH<sub>2</sub> and CH<sub>3</sub> groups (1462  $\text{cm}^{-1}$ ),  $\nu$  O-H bonds of hydroxyl groups (3018-3690  $\text{cm}^{-1}$ ); <sup>1</sup>H NMR (400 MHz, DMSO-*d*<sub>6</sub>):  $\delta$  0.69 (4H, [SiO<sub>1.5</sub>]<sub>n</sub>CH<sub>2</sub>-), -N<sup>+</sup>CH<sub>2</sub>CH<sub>2</sub>CH<sub>2</sub>-), 0.86 (3H, -CH<sub>3</sub>), 1.25 (12H, CH<sub>3</sub>(CH<sub>2</sub>)<sub>6</sub>-), 1.77 (4H, -N<sup>+</sup>CH<sub>2</sub>CH<sub>2</sub>-), 3.18, 3.38, 3.48 (16H, -N<sup>+</sup>CH<sub>2</sub>-), -CH<sub>2</sub>OH, -CH<sub>2</sub>OH, -CH(OH)-), 4.03 (2H, -CH(OH)-).

**Characterization.** FTIR spectra were recorded using a TENSOR 37 FT-IR spectrophotometer operated in 600-4000  $\text{cm}^{-1}$  range. <sup>1</sup>H NMR spectra were recorded with a Varian

VXR-400 MHz spectrometer using DMSO-*d*<sub>6</sub> (Cambridge Isotope Laboratories, Inc.) as solvent. The temperature dependence of the heat flow of the obtained compounds was studied by Q2000 (TA Instruments, USA) in the temperature range from -40 to 80 °C at a heating rate of 20 °C/min under a nitrogen atmosphere. The heating and cooling cycle was repeated twice and the data obtained during the second cycle was used to characterize the structure of the compound. The temperature of the onset of thermal oxidative degradation, which was taken as the temperature of 5% weight loss of the sample, was determined using Q50 (TA Instruments) in the temperature range from 20 to 700 °C at a heating rate of 20 °C/min in air. Self-assembly of OSS-ILs was studied in aqueous solutions at a concentration of 5 mg/ml. The OSS-IL particle size distribution in aqueous media was obtained based on a scattered light intensity study performed by dynamic light scattering (DLS) using a Zetasizer Nano ZS (Malvern) with Non-Invasive Back-Scatter (NIBS) technology (HeNe gas laser operating at a wavelength of 633 nm, scattering angle is 173°). The autocorrelation functions of the scattered light were calculated by the Malvern Zetasizer software. The values of  $\zeta$ -potential of OSS-IL particles in aqueous solution were determined by electrophoretic light scattering (ELS) on the Zetasizer Nano ZS (Malvern) by averaging three independent measurements from 35 scans. To study the morphology of OSS-IL assemblies, 100  $\mu$ L of an aqueous solution of OSS-IL was spin-casted onto a pre-cleaned silicon substrate (1.5 cm x 1.5 cm) at 3,000 rpm for 30 sec.

For the substrate cleaning, freshly cut [100] silicon substrates (University Wafer) were cleaned with piranha solution (2:1 concentrated sulfuric acid to hydrogen peroxide mixture, *caution: strong oxidizer!*) in accordance with established procedure. The substrates were thoroughly rinsed with ultrapure water and dried with a dry nitrogen gas.<sup>41</sup> The surface morphology of the spin-cast films was observed with an atomic force microscope (AFM) (ICON, Bruker) in the soft tapping mode. AFM probes (HQ:XSC11/AL BS, Mikromasch) were used with a spring constant of 7 N/m and a radius of 8 nm. The OSS-IL films were scanned at scanning rate of 0.5-1.0 Hz with the resolution of 512 x 512 or 1024 x 1024 pixels. PeakForce quantitative nanomechanical mapping (PF-QNM) was performed on AFM (ICON, Bruker) to investigate surface adhesion of the OSS-IL films. For PF-QNM, spring constants of AFM probe were determined. Deflection sensitivity of the AFM probes was determined from force-distance curves obtained on a sapphire crystal, and the spring constant was calculated using a thermal calibration method.<sup>42</sup> The scanning rate was kept at 0.5 Hz and the resolution was 512 x 512 pixels. All AFM images were processed and analyzed using Nanoscope Analysis v.2.0 software (Bruker). Ionic conductivity ( $\sigma_{dc}$ ) of the OSS-ILs was measured by the dielectric relaxation spectroscopy using a dielectric spectrometer based on a P5083 AC bridge scheme (0.1–100 kHz) and a two-electrode stainless steel cell (measurement accuracy of 0.03%). The samples were dried for 30 min at 100 °C under nitrogen flow before the measurements. The measurements were performed under a dry nitrogen atmosphere at a temperature from 40 to 120 °C.

### 3. Results and Discussion

#### 3.1 Synthesis and Characterizations of OSS-ILs

The initial OSS(N+OH) compound is a mixture of silsesquioxane nanoparticles, composed of an inorganic cages and open-chain structures and an organic component containing aliphatic hydroxyl and tertiary amino groups in the ratio N : OH = 1 : 4 (Figure 1).<sup>25, 26</sup> The size distribution of these nanoparticles is relatively narrow and their average size

measured by TEM is 2.7 nm, and this size corresponds to that of a single silsesquioxane-based nanoparticle consisting of 12–18 Si atoms.<sup>25</sup>

Amphiphilic reactive cationic aprotic OSS-ILs were synthesized by the reaction of quaternization of tertiary amino groups of OSS(N+OH) with 1-bromopropane or 1-bromodecane at the ratio N : Br = 1 : 1, resulting in the preparation of OSS(C<sub>3</sub>N<sup>+</sup>Br<sup>-</sup>) or OSS(C<sub>10</sub>N<sup>+</sup>Br<sup>-</sup>), respectively. The synthesized OSS-ILs exhibit different hydrophilic-hydrophobic balance due to different lengths of the introduced alkyl radical. They are viscous brown liquids, soluble in water, DMF, DMSO, insoluble in acetonitrile, acetone, ethyl acetate, hexane, chloroform, THF, diethyl ether, and toluene. OSS(C<sub>10</sub>N<sup>+</sup>Br<sup>-</sup>) dissolves in ethanol upon heating.

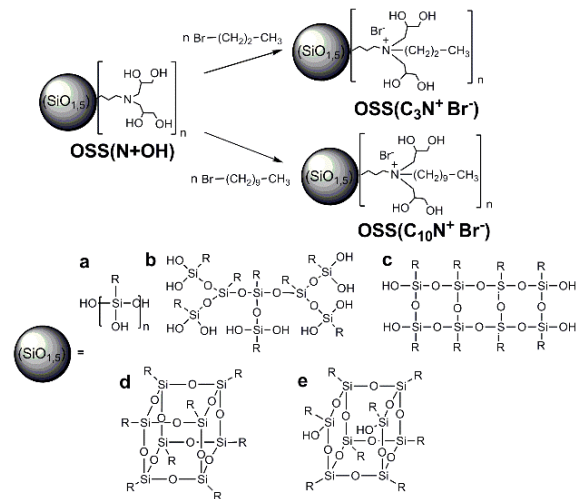


**Figure 1.** Scheme for the synthesis of reactive cationic OILs based on OSS(N+OH) and structures of the silsesquioxane core: linear (a), branched (b), completely condensed polyhedral nanostructures (d) and incompletely condensed polyhedral structures (e).

FTIR spectra of OSS(N+OH) and OSS-ILs are generally similar (Figure 2). They contain absorption bands of stretching vibrations of Si-O-Si bonds (1023–1043 cm<sup>-1</sup>), C-H bonds of CH, CH<sub>2</sub> and CH<sub>3</sub> groups (2765–3020 cm<sup>-1</sup>), OH bonds of hydroxyl groups (3018–3723 cm<sup>-1</sup>), deformation vibrations of C-H bonds of CH, CH<sub>2</sub> and CH<sub>3</sub> groups (1462–1463 cm<sup>-1</sup>). At the same time, the synthesized OSS-ILs contain alkyl chains of various lengths covalently bound to the quaternary ammonium atom in the organic shell. In this regard, an increase in the relative intensities of the absorption bands corresponding to the stretching vibrations of C-N bonds (1097–1120 cm<sup>-1</sup>) is observed in the IR spectra of OSS-ILs.<sup>43</sup>

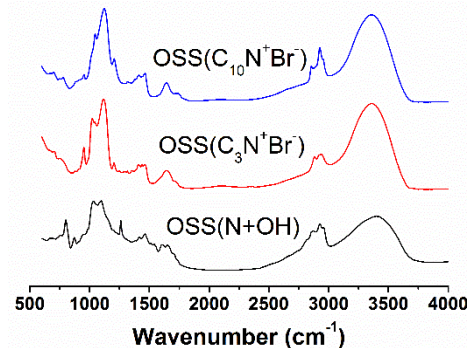


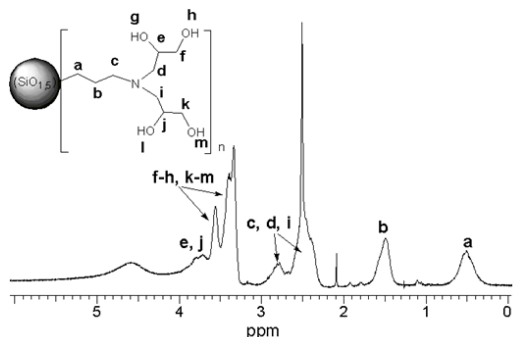
**Figure 2.** FTIR spectra of OSS(N+OH) and OSS-ILs.

The <sup>1</sup>H NMR spectrum of the initial compound OSS(N+OH) (Figure 3a) contains signals of the protons of the

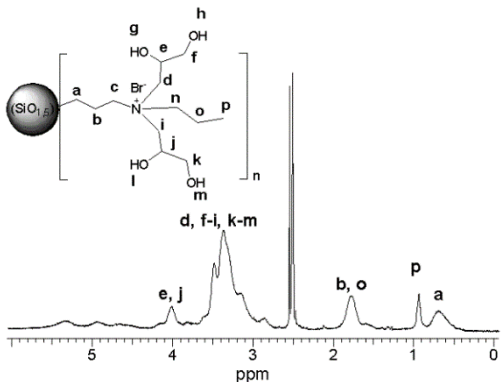
CH<sub>2</sub> groups at  $\alpha$ - (2.38 and 2.78 ppm),  $\beta$ - (1.50 ppm) and  $\gamma$ - (0.51 ppm) positions to the tertiary nitrogen atom, signals of the protons of CH and CH<sub>2</sub> groups in the  $\alpha$ -position to hydroxyl groups and signals of protons of hydroxyl groups in the range of 3.25-4.00 ppm.<sup>43</sup>

In the OSS-ILs spectra (Figures 3b and 3c), the signals of the protons of CH<sub>2</sub> groups in the  $\alpha$ -position towards nitrogen atoms are shifted towards the weak field (3.37 ppm for OSS(C<sub>3</sub>N<sup>+</sup>Br<sup>-</sup>) and 3.38 ppm for OSS(C<sub>10</sub>N<sup>+</sup>Br<sup>-</sup>)), compared with those in the OSS(N+OH) spectrum. In addition, signals of CH<sub>3</sub> group protons appear (0.94 ppm for OSS(C<sub>3</sub>N<sup>+</sup>Br<sup>-</sup>) and 0.86 ppm for OSS(C<sub>10</sub>N<sup>+</sup>Br<sup>-</sup>)), as well as repeating CH<sub>2</sub> groups of the alkyl chain attached to the nitrogen atom during quaternization for OSS(C<sub>10</sub>N<sup>+</sup>Br<sup>-</sup>) (1.25 ppm).

**a**



**b**



**c**

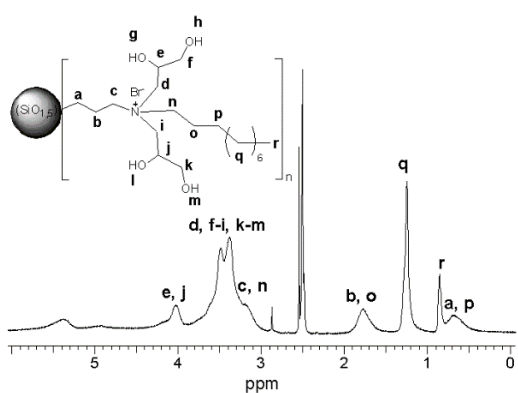


**Figure 3.** <sup>1</sup>H NMR spectra of OSS(N+OH) (a), OSS(C<sub>3</sub>N<sup>+</sup>Br<sup>-</sup>) (b) and OSS(C<sub>10</sub>N<sup>+</sup>Br<sup>-</sup>) (c).

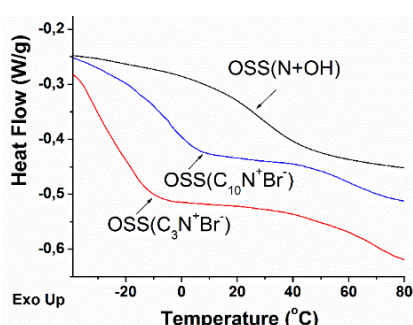
### 3.2 Thermal properties

According to DSC data (Figure 4a), the initial OSS(N+OH) and obtained OSS-ILs are amorphous substances. The glass transition temperature (T<sub>g</sub>) of the initial OSS(N+OH) is 25 °C<sup>44</sup> (Table 1). The introduction of ionic groups and aliphatic substituents into its organic shell shifts the T<sub>g</sub> value to below 0 °C. T<sub>g</sub> of OSS(C<sub>3</sub>N<sup>+</sup>Br<sup>-</sup>) and OSS(C<sub>10</sub>N<sup>+</sup>Br<sup>-</sup>) is -25°C

and -4°C respectively (Table 1), which are lower than those of the aprotic ammonium OSS-IL (T<sub>g</sub> OSS-IL = 15 °C<sup>29, 31</sup>) or POSS-ILs (2.73 °C and 24.6 °C<sup>17</sup>) reported in the literature. The lower T<sub>g</sub> for OSS(C<sub>3</sub>N<sup>+</sup>Br<sup>-</sup>) with shorter alkyl radical as compared to that for OSS(C<sub>10</sub>N<sup>+</sup>Br<sup>-</sup>) is associated with decrease in the intensity of intermolecular interactions and corresponding decrease in the rigidity and packing density.<sup>17, 45-47</sup> The cohesive interaction increases with an increase in the length of the alkyl radical due to the more intense hydrophobic interaction between the alkyl fragments.<sup>48-50</sup>

The introduction of short alkylurethane fragments into the branched organic shell of the initial nonionic OSS(N+OH) by the reaction of hydroxyl groups with n-butyl isocyanate led to a decrease in T<sub>g</sub> from 25 °C to 17 °C.<sup>44</sup> A further increase in the length of the alkyl chains achieved through the introduction of n-octadecylurethane compounds led to a significant increase in the T<sub>g</sub> value up to 53 °C due to the enhancement of hydrophobic interactions.<sup>44</sup> This also leads to the formation of a crystalline phase with T<sub>m</sub> of 82 °C.<sup>44</sup> The effect of increasing T<sub>g</sub> with increasing the length of alkyl substituent is also observed for OSS-ILs based on the OSS(N+OH) described in this work (Table 1).

**a**



**b**

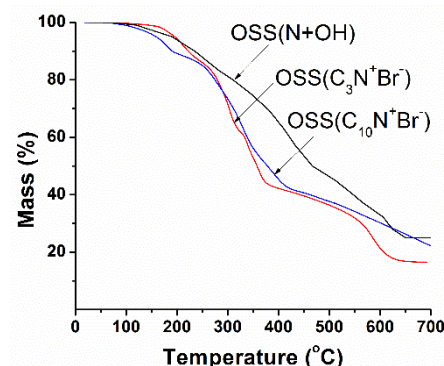


**Figure 4.** DSC (a) and TGA (b) curves for OSS(N+OH) and OSS-IL.

The effect of replacing the octahedral core of POSS containing trimethylammonium bis (trifluoromethanesulfonyl) imide group in an organic shell with the corresponding OSS mixture was studied in literature.<sup>29, 30</sup> The octahedral ionic aprotic POSS is a crystalline compound with a melting point of 172 °C (T<sub>m</sub>) but its analogue with a core in the form of OSS mixture is an amorphous compound with a glass transition temperature of 15 °C and can be classified as an ionic liquid. The replacement of ammonium with 1-methylimidazolium cations for the compounds with POSS core results in decreasing the value of T<sub>m</sub> down to 105 °C and appearance of amorphous phase with T<sub>g</sub> of -22 °C.<sup>30</sup> It should be noted that OSS with 1-methylimidazolium cations is an amorphous substance with T<sub>g</sub> of -25 °C, which is an evidence of its ionic liquid nature.<sup>30</sup> In addition, the combination of ammonium and

**Table 1.** Characteristics of OSS(N+OH), OSS-ILs and their aqueous solutions

Samples	M <sub>n</sub> theor* (g/mol)	Content of ionic groups, meq/g	T <sub>g</sub> , °C		Size, (DLS) (nm)	Zeta potential (mV)	σ <sub>dc</sub> , S/cm			
			T <sub>g</sub> , °C	T <sub>d5%</sub> , °C			40 °C	80 °C	100 °C	120 °C
OSS(N+OH)	4040	-	25	190						
OSS(C <sub>3</sub> N <sup>+</sup> Br <sup>-</sup> )	6000	2.63	-25	195	152±7	+62.9±3.4	3·10 <sup>-5</sup>	2.4·10 <sup>-4</sup>	6.7·10 <sup>-4</sup>	1.4·10 <sup>-3</sup>
OSS(C <sub>10</sub> N <sup>+</sup> Br <sup>-</sup> )	7570	2.09	-4	158	165±16	+52.0±3.5	2.2·10 <sup>-8</sup>	3.6·10 <sup>-6</sup>	1.2·10 <sup>-5</sup>	1.3·10 <sup>-4</sup>

\* Calculated on the basis of MM OSS(N+OH)<sup>26</sup> and MM of organic shell.

1-methylimidazolium ionic groups in the organic frame of octahedral POSS completely suppresses the crystallization process which leads to its transition to the state of ionic liquid.<sup>31</sup> The T<sub>g</sub> value of this compound increases to -8 °C, in comparison with octahedral imidazolium-containing POSS compounds.<sup>31</sup> The OSS-IL with the same combination of ammonium and imidazolium ionic groups is also an amorphous substance with a T<sub>g</sub> value of -10 °C.<sup>31</sup>

As was reported, the nature of counterions has a significant effect on the structure of cationic aprotic octahedral POSS. Transitions related to the melting of the crystalline phase or glass transition of the amorphous phase were not observed in the range from -90 °C to 120 °C for POSS containing iodides of trimethyl-, tri-n-butyl- or tri-n-octyl-ammonium groups.<sup>17</sup> Replacement of the iodine anions with bis(trifluoromethanesulfonyl) imide anions leads to the appearance of glass transition.<sup>17</sup> The T<sub>g</sub> value decreases from 25 °C for POSS with methyl substituent at the quaternary nitrogen atom to about 3°C for POSS with n-butyl substituent.<sup>17</sup>

According to TGA data, the temperature of the onset of decomposition (T<sub>d5%</sub>) of the compound with the shorter alkyl substituent, OSS(C<sub>3</sub>N<sup>+</sup>Br<sup>-</sup>) is close to that of the initial OSS(N+OH). (Figure 4b, Table 1). For OSS(C<sub>10</sub>N<sup>+</sup>Br<sup>-</sup>) with longer alkyl substituent, the T<sub>d5%</sub> value significantly decreases. Thermal stability of the synthesized OSS-ILs is close to ionic POSS with iodide anions (207-253 °C)<sup>17</sup> but much lower than ionic POSS and OSS containing thermally stable (CF<sub>3</sub>SO<sub>2</sub>)<sub>2</sub>N<sup>-</sup> anions (417-420 °C).<sup>31</sup> On the other hand, the presence of ionic groups in the obtained OSS-ILs significantly reduces their resistance to thermal oxidative degradation in comparison with alkylurethane-containing non-ionic POSS with the same composition of the inorganic component.<sup>44</sup> The decrease in thermal stability of OSS(C<sub>10</sub>N<sup>+</sup>Br<sup>-</sup>) compared to that of the initial oligomer OSS(N+OH) confirms the quaternization of tertiary amino groups by bromodecane and the formation of ionic centers.

### 3.3 Colloidal properties of OSS-ILs

The behavior of the OSS-ILs in aqueous media were investigated by the DLS showed bimodal size distribution for OSS(C<sub>3</sub>N<sup>+</sup>Br<sup>-</sup>) with an average size of aggregates of 152 ± 7 nm (Figure 5a).

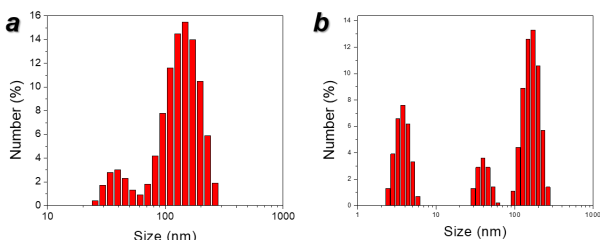


**Figure 5.** Size distribution of OSS(C<sub>3</sub>N<sup>+</sup>Br<sup>-</sup>) (a) and OSS(C<sub>10</sub>N<sup>+</sup>Br<sup>-</sup>) (b) assemblies in aqueous solutions.

A different aggregation is observed for the aqueous solution of OSS(C<sub>10</sub>N<sup>+</sup>Br<sup>-</sup>). OSS(C<sub>10</sub>N<sup>+</sup>Br<sup>-</sup>) showed multimodal size distribution with three peaks (Figure 5b). This result suggests that the length of alkyl substituent of OSS-ILs affects the assembly behavior in aqueous solutions, resulting in the formation of more diverse morphologies with longer alkyl substituent.

The surface morphology of OSS-IL films obtained by spin-casting from solution was studied using AFM (Figure 6). Spherical flat micelles were formed from OSS(C<sub>3</sub>N<sup>+</sup>Br<sup>-</sup>) with an average diameter of 229 ± 92 nm and an average height of 2 nm (Figure 6a-d). On the other hand, the AFM images of OSS(C<sub>10</sub>N<sup>+</sup>Br<sup>-</sup>) films show polydisperse micellar morphologies, which is in good agreement with the DLS result, and a majority of the morphologies exhibit elongated, micron long worm-like structures with an average height of 2 nm (Figure 6e-h). Such difference in surface morphology between these two OSS-IL films can be explained by variation in hydrophobicity of OSS-ILs depending on the length of alkyl substituent. The morphological transition from spherical to worm-like micelles have been reported for amphiphilic polymers by increasing their hydrophobicity.<sup>56, 57</sup>

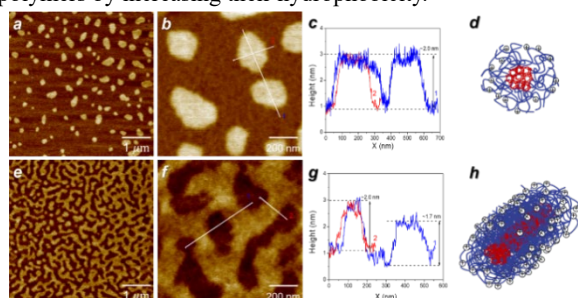


**Figure 6.** AFM topography images of spin-cast films of OSS(C<sub>3</sub>N<sup>+</sup>Br<sup>-</sup>) (a-b) and OSS(C<sub>10</sub>N<sup>+</sup>Br<sup>-</sup>) (e-f) and the corresponding height profiles along the indicated lines (c and g). Z scale of all AFM images is 5 nm. (d-h) Schematic representation of OSS(C<sub>3</sub>N<sup>+</sup>Br<sup>-</sup>) (g) and OSS(C<sub>10</sub>N<sup>+</sup>Br<sup>-</sup>) (h) assemblies.

In addition, mapping of surface adhesion of the OSS-IL morphologies was investigated by performing PF-QNM imaging (Figure 7). The surface of spherical flat domains of OSS(C<sub>3</sub>N<sup>+</sup>Br<sup>-</sup>) show much higher adhesion compared to interdomain region (Figure 7b). On the other hand, OSS(C<sub>10</sub>N<sup>+</sup>Br<sup>-</sup>) morphologies show no remarkable contrast in surface adhesion between the worm-like domains and interdomain region (Figure 7d). As mentioned earlier, the hydrophobicity of OSS-ILs increase with longer alkyl substitutes, resulting in the decreased adhesion with hydrophilic AFM probes.<sup>42, 58</sup> This result indicates that not only morphology but also surface mechanical deformational response (surface stiffness) can be tuned by adjusting the length of alkyl substitutes of OSS-ILs.

The high values of the  $\zeta$ -potential of the OSS( $C_3N^+Br^-$ ) and OSS( $C_{10}N^+Br^-$ ) particles in aqueous solution according to ELS data (Table 1) can be associated with the presence of positively charged quaternary ammonium terminal groups on their surface. The lower value of  $\zeta$ -potential of the OSS( $C_{10}N^+Br^-$ ) particles as compared to OSS( $C_3N^+Br^-$ ) is probably due to the longer length of the alkyl substituent at the quaternary nitrogen atom and charge screening. Since colloidal systems with  $\zeta$ -potential values above 30 mV in modulus are considered as a high stable system<sup>59</sup>, the OSS( $C_3N^+Br^-$ ) and OSS( $C_{10}N^+Br^-$ ) particles are resistant to aggregation in an aqueous solution.

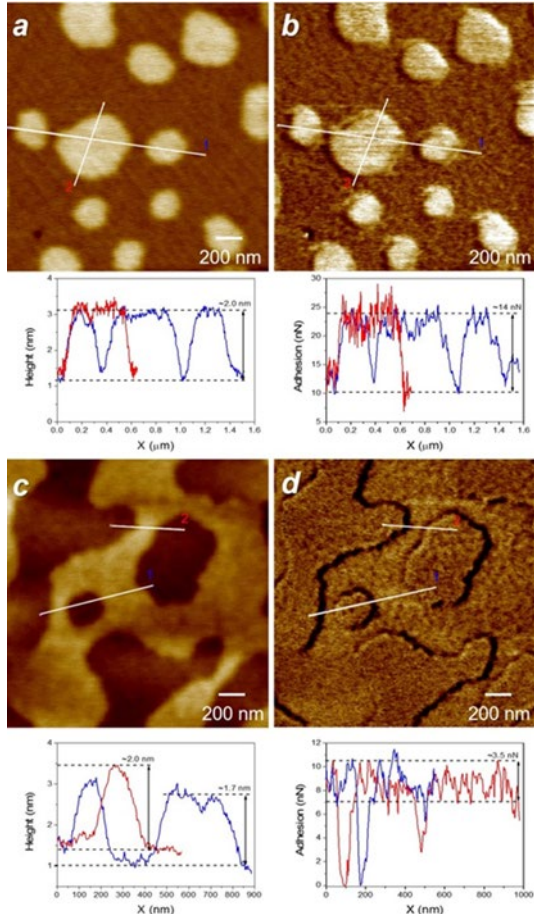


**Figure 7.** Topography (a,c) and adhesion (b,d) images and corresponding profiles of the OSS( $C_3N^+Br^-$ ) (a,b) and OSS( $C_{10}N^+Br^-$ ) (c-d) films. Z scale is 5 nm for (a,c), 30 nN for (b) and 15 nN for (d).

### 3.4 Ionic conductivity

One of the most intriguing applications of polymer analogs of ionic liquids is the development of electrolytes for various electrochemical devices.<sup>51-53</sup> Based on the structure of the synthesized OSS-ILs, they can be classified as electrolytes with a single-ion conduction mechanism provided mainly by  $Br^-$  anions. In this work, we investigated the dc conductivity ( $\sigma_{dc}$ ) of these compounds under anhydrous conditions in the temperature range of 40–120 °C. An increase in the value of  $\sigma_{dc}$  with increasing temperature indicates ionic nature of conductivity (Figure 8, Table 1).<sup>54</sup> The conductivity of OSS( $C_3N^+Br^-$ ) is higher compared to OSS( $C_{10}N^+Br^-$ ) due to the higher mobility of charge carriers in its composition.

As the temperature rises, the conductivity of OSS( $C_{10}N^+Br^-$ ) increases intensively in comparison to OSS( $C_3N^+Br^-$ ). The difference in  $\sigma_{dc}$  values between these two compounds at 40 °C is three orders of magnitude and at 120 °C

only by one order of magnitude. The achieved maximum value of  $\sigma_{dc}$  is  $1.4 \cdot 10^{-3}$  S/cm for OSS( $C_3N^+Br^-$ ). It should be noted that there is a correlation between the  $T_g$  and conductivity of OSS-ILs. In fact, OSS( $C_3N^+Br^-$ ) has a higher conductivity and lower  $T_g$  compared to OSS( $C_{10}N^+Br^-$ ).

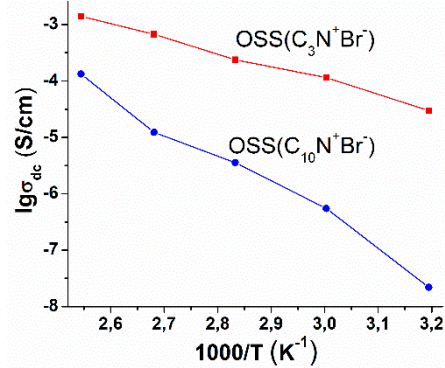


**Figure 8.** Temperature dependence of conductivity of OSS-ILs.

There is practically no difference in ionic conductivity between a compound with a polyhedral structures and a compound bearing imidazolium bis (trifluoromethanesulfonyl) imide group with a mixed one (OSS-IL).<sup>30</sup> At 100 °C, the value of their  $\sigma_{dc}$  is in the range of  $10^{-4} - 10^{-3}$  S/cm. This level is close to that for the OSS-IL compounds synthesized in this work. The octafunctional aprotic POSS containing trimethyl-substituted n-propylammonium fragments with bis (trifluoromethanesulfonyl) imide counterions<sup>31</sup> is not considered as a conductive material because of the high  $T_m$  value (172 °C). A compound with the same organic shell based upon a mixture of silsesquioxane structures is comparable to conventional ionic liquids with conductivity range of  $10^{-8}$  to  $10^{-4}$  S/cm in the range 20–100 °C.<sup>30</sup>

### 4. Conclusion

A method for producing organic-inorganic amphiphilic reactive aprotic cationic ionic liquids based on the quaternization reaction of a mixture of oligosilsesquioxane polyhedral structures and their analogs with an open chain containing a tertiary amine and primary and secondary hydroxyl groups in an organic shell with *n*-bromopropane or *n*-bromodecane has been suggested. These compounds are the representatives of the amphiphilic aprotic cationic OSS-ILs, capable of polycondensation reactions. They are amorphous with  $T_g$  below 0 °C.

In aqueous solutions, an increase in the hydrophobicity of the synthesized OSS-ILs leads to an increase in the polydispersity of size distribution of their assemblies. Their average size is 150–170 nm. At the same time, the high values of their  $\zeta$ -potentials indicate a high aggregate stability. A different character of self-organization of OSS-ILs is observed in a condensed state in an ultrathin film on a solid silicon substrate. The compound OSS( $C_3N^+Br^-$ ) forms disk-like structures with a diameter of several hundred nanometers and a thickness of 2 nm. The compound with higher hydrophobicity, OSS( $C_{10}N^+Br^-$ ) forms worm-like structures with the same thickness of 2 nm. Surface properties mapping shows that not only surface morphology but also surface mechanical and adhesive responses can be tuned by adjusting the amphiphilicity of OSS-ILs.

The ionic conductivity of the synthesized compounds is comparable to that of traditional imidazolium-containing POSS with the increase in length of the alkyl substituent leading to a decrease in the conductivity. Meanwhile, as the temperature rises, the conductivity of OSS( $C_{10}N^+Br^-$ ) increases more

intensively compared to OSS( $C_3N^+Br^-$ ). Finally, the lower  $T_g$ , facilitates higher ionic conductivity with maximum conductivity value of the OSS-ILs achieved of  $1.4 \cdot 10^{-3}$  S/cm at 120 °C.

In conclusion, the organization and properties of OSS-ILs are controlled by the structure of their ionic group and its content, as well as by the structure of the organic shells as a whole. In particular, the ionic conductivity of OSS-ILs gives these materials great potential as polymer electrolytes for various electrochemical applications, such as sensors.

### Acknowledgement

The authors thank the staff of the Center the scientific equipment “Research Station to study the thermal and mechanical properties of polymeric materials” NAS of Ukraine at the Institute of Macromolecular Chemistry of the NAS of Ukraine for thermophysical research by differential scanning calorimetry (DSC) and thermogravimetric analysis (TGA).

This study was financially supported by the target program of fundamental studies of the NAS of Ukraine “New Functional Substances and Materials of Chemical Production” and by the National Science Foundation, DMR 2001968.

### References

1. J. Dupont, R. F. de Souza, P. A. Z. Suarez, *Chem. Rev.* **2002**, *102*, 3667..
2. A.S. Shaplov, D.O. Ponkratov, Ya.S. Vygodskii, *Polym. Sci.* **2016**, *58*, 73.
3. D. Mecerreyres, *Prog. Polym. Sci.* **2011**, *36*, 1629.
4. A.S. Shaplov, D.O. Ponkratov, P.S. Vlasov, E.I. Lozinskaya, L.I. Komarova, I.A. Malyshkina, F. Vidal, G.T.M. Nguyen, M. Armand, C. Wandrey, Ya.S. Vygodskii, *Polym. Sci. Ser. B* **2013**, *55*, P. 122.
5. V.V. Shevchenko, A.V. Stryutsky, N.S. Klymenko, M.A. Gumennaya, A.A. Fomenko, V.N. Bliznyuk, V.V. Trachevsky, V.V. Davydenko, V.V. Tsukruk, *Polymer* **2014**, *55*, 3349.
6. V.V. Shevchenko, A.V. Stryutsky, N.S. Klymenko, M.A. Gumennaya, A.A. Fomenko, V.V. Trachevsky, V.V. Davydenko, V.N. Bliznyuk, A.V. Dorokhin, *Polym. Sci. Ser. B* **2014**, *56*, 583.
7. K. Tanaka, Y. Chujo, *J. Mater. Chem.* **2012**, *22*, 1733.
8. K. Tanaka, Y. Chujo, *Bull. Chem. Soc. Jpn.* **2013**, *86*, 1231.
9. Y. Kaneko, M. Shoiriki, T. Mizumo, *J. Mater. Chem.* **2012**, *22*, 14475.
10. Q. Zou, Q. Yan, G. Song, S. Zhang, L. Wu, *Biosens. Bioelectron.* **2007**, *22*, 1461.
11. T. Tokunaga, M. Shoiriki, T. Mizumo, Y. Kaneko, *J. Mater. Chem. C* **2014**, *2*, 2496.
12. K. Tanaka, F. Ishiguro, Y. Chujo, *J. Am. Chem. Soc.* **2010**, *132*, 17649.
13. J. Jeon, K. Tanaka, Y. Chujo, *RSC Advances.* **2013**, *3*, 2422.
14. V. Elumalai, S. Dharmalingam, *Polym. Compos.* **2019**, *40*, 1536.
15. M. Čolović, J. Volavšek, E. Stathatos, N. Čelan Korošin, M. Šobak, I. Jerman, *Sol Energy* **2019**, *183*, 619.
16. S.B. Burujeny, H. Yeganeh, M. Atai, H. Gholami, M. Sorayya, *Dent Mater.* **2017**, *33*, 119.
17. S. Manickam, P. Cardiano, P.G. Mineo, S. Lo Schiavo, *Eur. J. Inorg. Chem.* **2014**, 2704.
18. P. Majumdar, E. Lee, N. Gubbins, S.J. Stafslien, J. Daniels, C.J. Thorson, B.J. Chisholm, *Polymer* **2009**, *50*, 1124.
19. P. Majumdar, J. He, E. Lee, A. Kallam, N. Gubbins, S.J. Stafslien, J. Daniels, B.J. Chisholm, *J. Coat. Technol. Res.* **2010**, *7*, 455.
20. Y. Liu, C. Leng, B. Chisholm, S. Stafslien, P. Majumdar, Z. Chen, *Langmuir* **2013**, *29*, 2897.
21. J. Chojnowski, W. Fortuniak, P. Rościszewski, W. Werel, J. Łukasiak, W. Kamysz, R. Hałasa, *J. Inorg. Organomet. Polym. Mater.* **2006**, *16*, 219.
22. F. Dong, L. Lu, C. Ha, *Macromol. Chem. Phys.* **2019**, 1800324.
23. F. Chen, F. Lin, Q. Zhang, R. Cai, Y. Wu, X. Ma, *Macromol. Rapid Commun.* **2019**, 1900101.
24. H. Zhou, Q. Yea, J. Xu, *Mater. Chem. Front.* **2017**, *1*, 212.
25. H. Mori, M.G. Lanzendorfer, A.H.E. Müller, J.E. Klee, *Macromolecules* **2004**, *37*, 5228.
26. R. Gunawidjaja, F. Huang, M. Gumenna, N. Klimenko, G.A. Nunnery, V. Shevchenko, R. Tannenbaum, V.V. Tsukruk, *Langmuir* **2009**, *25*, 1196.
27. L. Matějka, O. Dukh, J. Brus, W.J. Simonsick, B. Meissner, *J. Non Cryst. Solids* **2000**, *270*, 34.
28. P. Eisenberg, R. Erra-Balsells, Y. Ishikawa, J.C. Lucas, A.N. Mauri, H. Nonami, C.C. Riccardi, R.J.J. Williams, *Macromolecules* **2000**, *33*, 1940.
29. T. Ishii, T. Mizumo, Y. Kaneko, *Bull. Chem. Soc. Jpn.* **2014**, *87*, 155.
30. T. Ishii, T. Enoki, T. Mizumo, J. Ohshita, Y. Kaneko, *RSC Adv.* **2015**, *5*, 15226.
31. A. Harada, S. Koge, J. Ohshita, Y. Kaneko, *Bull. Chem. Soc. Jpn.* **2016**, *89*, 1129.
32. S. Muthukrishnan, F. Plamper, H. Mori, A.H.E. Müller, *Macromolecules* **2005**, *38*, 10631.
33. F.A. Plamper, A. Schmalz, E. Penott-Chang, M. Drechsler, A. Jusufi, M. Ballauff, A.H.E. Müller, *Macromolecules* **2007**, *40*, 5689.
34. F.A. Plamper, M. Ruppel, A. Schmalz, O. Borisov, M. Ballauff, A.H.E. Müller, *Macromolecules* **2007**, *40*, 8361.
35. I. Choi, R. Suntivich, F.A. Plamper, C.V. Synatschke, A.H.E. Müller, V.V. Tsukruk, *J. Am. Chem. Soc.* **2011**, *133*, 9592.
36. W. Xu, P.A. Ledin, F.A. Plamper, C.V. Synatschke, A.H.E. Müller, V.V. Tsukruk, *Macromolecules* **2014**, *47*, 7858.
37. M. Schumacher, M. Ruppel, J. Kohlbrecher, M. Burkhardt, F. Plamper, M. Drechsler, A.H.E. Müller, *Polymer* **2009**, *50*, 1908.
38. W. Li, D. Wang, D. Han, R. Sun, J. Zhang, S. Feng, *Polymers* **2018**, *10*, 917.
39. W. Li, S. Feng, *J. Mol. Liq.* **2018**, *265*, 269.
40. M. Dule, M. Biswas, T.K. Paira, T.K. Mandal, *Polymer*, **2015**, *77*, 32.
41. W. Xu, P. A. Ledin, Z. Iatridi, C. Tsitsilianis, V. V. Tsukruk, *Macromolecules* **2015**, *48*, 3344.
42. H. Lee, A. V. Stryutsky, V. F. Korolovych, E. Mikan, V. V. Shevchenko, V. V. Tsukruk, *Langmuir* **2019**, *35*, 11809.
43. E. Pretsch, Ph. Bühlmann, M. Badertscher, Structure determination of organic compounds. Tables of spectral data. 4<sup>th</sup> Edition Springer-Verlag, 2009.
44. V. V. Shevchenko, M. A. Gumennaya, A. V. Shevchuk, Yu. P. Gomza, N. S. Klimenko, V. V. Boichuk, *Polym. Sci. Ser. B* **2009**, *51*, 46.
45. D. Maeda, T. Ishii, Y. Kaneko, *Bull. Chem. Soc. Jpn.* **2018**, *91*, 1112.
46. T. L. Greaves, C. J. Drummond, *Chem. Rev.* **2008**, *108*, 206.

47. T. L. Greaves, C. J. Drummond, *Chem. Rev.* **2015**, *115*, 11379.

48. J. M. S. S. Esperança, M. Tariq, A. B. Pereiro, J. M. M. Araújo, K. R. Seddon, L. P. N. Rebelo, *Front Chem.* **2019**, *7*, 450.

49. K. Goossens, K. Lava, C.W. Bielawski, K. Binnemans. *Chem. Rev.* **2016**, *116*, 4643.

50. F. Xu, K. Matsumoto, R. Hagiwara. *Chem. Eur. J.* **2010**, *16*, 12970.

51. A.S. Shaplov, R. Marcilla, D. Mecerreyes. *Electrochim. Acta.* **2015**, *175*, 18.

52. M. Watanabe, M. L. Thomas, S. Zhang, K. Ueno, T. Yasuda, K. Dokko, *Chem. Rev.* **2017**, *117*, 7190.

53. C. Lee, K. Ho. *European Polymer Journal.* **2018**, *108*, 420.

54. A. Kyritsis, P. Pissis, J. Grammatikakis, *J. Polym. Sci., Part B: Polym. Phys.* **1995**, *33*, 1737.

55. W. Xu, P. A. Ledin, V. V. Shevchenko, V. V. Tsukruk, *ACS Appl Mater Interfaces.* **2015**, *7*, 12570.

56. R. Renyves, M. Schmutz, I. J. Horner, F. V. Bright, J. Rzayev. *J. Am. Chem. Soc.* **2014**, *136*, 7762.

57. C. Li, Q. Li, Y. V. Kaneti, D. Hou, Y. Yamauchi, Y. Mai, *Chem. Soc. Rev.* **2020**, *49*, 4681.

58. V. Vadillo-Rodriguez, H. J. Busscher, H. C. van der Mei, J. de Vries, W. Norde. *Colloids Surfaces B: Biointerfaces.* **2005**, *41*, 33.

59. A. Kumar, C.K. Dixit, Methods for characterization of nanoparticles, in: S. Nimesh, R. Chandra, N. Gupta (Eds.), *Advances in Nanomedicine for the Delivery of Therapeutic Nucleic Acids*, Elsevier, 2017, 43.

## Graphical Abstract

Reactive amphiphilic aprotic ionic liquids based on functionalized oligomeric silsesquioxanes

Valery V. Shevchenko, Mariana Gumenna, Hansol Lee, Nina Klimenko, Oleksandr Stryutsky, Volodymyr Korolovych, Vladimir V. Tsukruk

A method for synthesis of organo-inorganic amphiphilic reactive aprotic cationic ionic liquids (OSS-ILs) was proposed. It was based on the quaternization reaction of oligomeric silsesquioxanes containing tertiary amine and hydroxyl groups in an organic shell with *n*-bromopropane or *n*-bromodecane. The influence of a structure of OSS-ILs on their thermal properties, ionic conductivity and peculiarities of self-organization was investigated.

